Using Electronic Coherence to Probe a Deeply Embedded Quantum Well in Bimetallic Pb/Ag Films on Si(111)

M. K. Brinkley, Y. Liu, N. J. Speer, T. Miller, and T.-C. Chiang

Department of Physics, University of Illinois at Urbana-Champaign, 1110 West Green Street, Urbana, Illinois 61801-3080, USA
Frederick Seitz Materials Research Laboratory, University of Illinois at Urbana-Champaign, 104 South Goodwin Avenue, Urbana, Illinois 61801-2902, USA

(Received 7 July 2009; published 7 December 2009)

We report an experiment in which we utilize electronic coherence to probe a deeply embedded thin film as a quantum well. An atomically uniform Ag film prepared on Si(111) was covered by Pb films up to 70 Å thick, and the resulting electronic structure was examined by angle-resolved photoemission spectroscopy. Despite a photoemission escape depth of just a few Ångströms and an incommensurate Pb/Ag interface, the data reveal a striking Fabry-Pérot-like structure characteristic of an Ag etalon buried deeply under the Pb overlayers. Our simulations clearly illustrate the manifest coherence of the electronic structures, permitting the characterization of the embedded Ag quantum well.

DOI: 10.1103/PhysRevLett.103.246801 PACS numbers: 73.21.Fg, 73.20.At, 79.60.Dp

Characterizing quantum-electronic behavior in buried layers of thin-film systems constitutes an outstanding issue in condensed-matter physics and electronic materials engineering. Though the study of buried structures is of basic importance to thin-film applications, surface-sensitive measurement techniques such as angle-resolved photoemission spectroscopy (ARPES) probe electrons within just the first few Ångströms of a material's surface, rendering them unable to access underlying structures directly. Moreover, the incommensurate interfaces and roughness of intervening films in multilayer systems can obscure the electronic properties of the submerged media [1]. Consequently, investigations of such systems have generally failed to assess the impact of constituent layers on the encompassing system. Using results obtained with ARPES, we remedy this shortcoming by examining the manifestation of interfering electrons in atomically uniform Ag films on Si(111) covered by Pb films of various thicknesses.

The confinement of electrons in a smooth film by its surface and interface gives rise to distinct electronic states known as quantum-well states when the thickness of the film approaches the nanoscale [2–5]. An archetypal quantum-well system is Ag on Si(111) (Ref. [1]). Akin to the standing waves in an optical Fabry-Pérot interferometer, electrons in the Ag film undergo mirrorlike reflections at the film surface and substrate-film interface that lead to discrete interferometer modes [6,7]. Similar modes are expected for films buried deeply under an overlayer. When a Pb slab is joined to an Ag slab, the Ag and Pb electronic structures coherently couple, analogous to a two-layer Fabry-Pérot interferometer. Despite a short photoelectron escape depth, the initial-state wave function sensed by photoemission propagates throughout both the Pb and Ag films due to a long phase-coherence length (i.e., a long mean-free-path [8,9]). The large lattice mismatch at the Ag/Si and Pb/Ag interfaces notwithstanding, this long electron coherence length promotes quantum interference and gives rise to an electronic structure characteristic of the entire system. The reflectivities of the Pb/Ag and Ag/Si interfaces, in addition to the phase shifts these interfaces influence, provide crucial information about an otherwise inaccessible quantum-well structure and the impact of its interfaces on electronic behavior in the films.

For our experiment, a Si(111)-(7×7) surface was prepared under ultrahigh-vacuum conditions and maintained at 50 K. Ag was then evaporated onto the Si substrate, annealed to room temperature, and cooled back to 50 K to yield an atomically uniform film of desired thickness and bulklike lattice constant [6]. Subsequently, Pb was deposited over this Ag film at 50 K, annealed to 120 K (well below the onset of thermal instability [10]), and cooled back to 50 K for photoemission measurements. The Pb film thicknesses quoted below are nominal thicknesses based on readings from a quartz thickness monitor calibrated for Ag deposition but corrected for the different material properties of Pb and Ag. All measurements were conducted *in situ* using 22-eV undulator radiation at the Synchrotron Radiation Center, University of Wisconsin-Madison. Acquired with a Scienta hemispherical analyzer, the photoemission spectra were recorded as two-dimensional images spanning the energy and polar emission angle. Each image covered a 10° range of emission angles. To cover the wider range of angles presented here, the sample was rotated in 6° increments to produce overlapping images, which were stitched together. The dispersion relations were measured along the $\bar{\Gamma}\bar{K}$ direction of the surface Brillouin zone.

The two-dimensional images in Fig. 1 are gray-scale representations of photoemission data for Si(111) covered first by p monolayers (ML) of Ag and then overcoated with q monolayers of Pb, where the values of p/q are shown for each case. The sharp, intense peak near normal emission

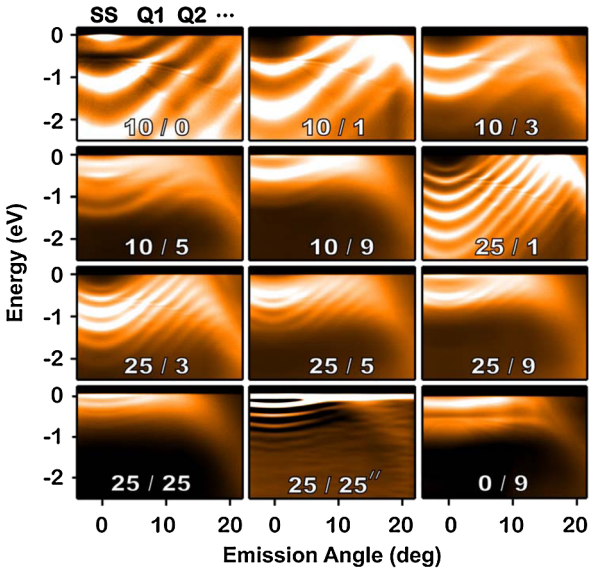

FIG. 1 (color online). Selected angle-resolved photoemission spectra (black represents low intensity) are displayed for Pb films on Ag films on Si(111). The notation p/q indicates a coverage of q ML of Pb on p ML of Ag, and the double-prime ($''$) denotes a second derivative with respect to the energy. The label "10/0," for example, represents a bare 10-ML Ag film on Si(111), while "0/9" signifies a bare 9-ML Pb film on Si(111).

($\theta = 0°$) and just below the Fermi level in the bare 10-ML Ag film spectrum ($p/q = 10/0$) owes to the Shockley surface state (denoted by SS) supported by the Ag(111) L gap. This surface state vanishes upon Pb coverage and is neglected in the ensuing analysis. The labels $Q1$, $Q2$, etc., refer to the quantum-well subbands in the bare Ag film, which are nearly parabolic about normal emission. These Ag dispersion curves are somewhat distorted near the Si substrate band edges by electronic coupling between the Ag and the Si substrate [11]. The data set corresponding to a 25-ML Ag film thickness shows a much denser set of quantum-well subbands than the 10 ML Ag film case, as expected.

These Ag subband structures remain visible after Pb coverage, but are otherwise modulated by the Pb emission. These spectral features, as will be shown below, derive from the Fabry-Pérot modes in the buried Ag that coherently couple to the photoemission process through the Pb film. To illustrate that electronic coherence persists even through thick overlayers of Pb, Fig. 1 includes a spectrum for a 25-ML Pb film on 25 ML Ag ($p/q = 25/25$) and its second derivative (labeled as $25/25''$) with respect to the energy. As evidenced in the 9-ML Pb/Si(111) spectrum ($p/q = 0/9$), the Pb quantum-well subbands are fairly flat near the zone center, while at larger emission angles they turn sharply downward [12]. Their relatively large linewidths afford the spectral setting for resolving the fine Ag-induced modulations.

One must first consider whether the Ag electronic structure superimposed on the Pb emission is the result of coherent or incoherent coupling. In the case of incoherent coupling, the photoemission intensity would be described by the sum of the intensities due to discrete Pb and Ag etalons, with an Ag contribution diminished exponentially by the Pb overlayer of thickness d_{Pb}:

$$I(E) = I_{\mathrm{Pb}}(E) + I_{\mathrm{Ag}}(E)\exp(-d_{\mathrm{Pb}}/\lambda). \quad (1)$$

The electronic mean-free-path λ in most metals at 22 eV is $\sim$2 ML of Pb(111) (Ref. [13]). A Pb coverage of 4 ML will therefore reduce the Ag contribution by $\sim$85%, effectively precluding the possibility that the Ag band structure is directly probed by photoemission. Furthermore, the Ag-like features present in the $p/q = 25/25$ case indicate that coherent electronic coupling persists through $\sim 12\lambda$, well beyond the direct reach of photoemission. The solid energy-distribution curves displayed in Fig. 2(a) represent the simulated results for electronically decoupled Pb/Ag films at normal emission for Pb films of various thicknesses on 25 ML Ag. Compared to the data (circles), the simu-

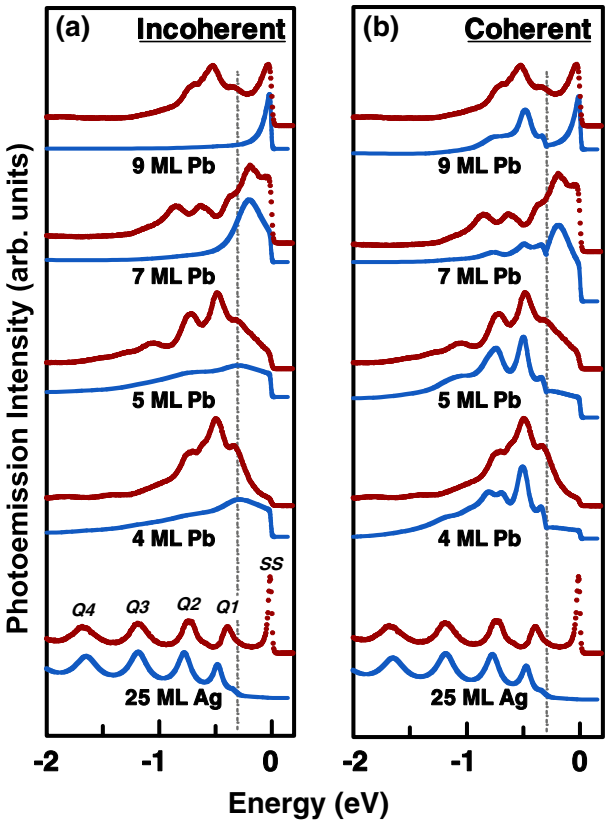

FIG. 2 (color online). (a) Cascaded normal-emission energy-distribution curves comparing the data (red circles) with the simulated results (blue curves) for incoherently coupled Pb films on an atomically uniform 25-ML Ag film on Si(111). (b) Similar comparison with simulated results for coherently coupled Pb films on a 25-ML Ag on Si(111). The vertical dashed lines indicate the position of the Ag valence-band maximum along (−0.3 eV).

lated results, dominated by the features of the Pb overlayer alone, fail to reveal the Ag-like features in the data.

The solid curves in Fig. 2(b) represent the results of simulations in which the Ag and Pb electronic wave functions are coherently coupled, and stem from the following analysis. The component of the electron Bloch wave vector along the surface-normal direction, $k_\perp(E)$, is determined by the Bohr-Sommerfeld quantization rule,

$$2k_\perp(E)Nt + \Phi(E) = 2n\pi, \tag{2}$$

where N denotes the number of monolayers, t the monolayer thickness, Φ the total boundary phase shift, and n a quantum number. The standard two-band model accurately characterizes the nearly free-electron-like sp bands of both Ag and Pb, wherefrom the dispersion relations are obtained [14–16].

Though the Bohr-Sommerfeld relationship specifies quantum-well peak positions, it does not yield spectral functions. A comprehensive examination of these spectra necessitates the consideration of the electronic wave functions [6]. As discussed in Ref. [6], the final state is a time-reversed low-energy-electron-diffraction (TRLEED) state. The initial state constitutes an electron inside the crystal heading toward the surface, which, upon photoexcitation into the TRLEED state, enters the detector and completes its circuit [1,6]. The initial state is subjected to a series of partial reflections between the film boundaries, which yields a Fabry-Pérot-like modulation. Extending this approach to include two layers (see, for example, Ref. [17]) generates a modulation factor given by

$$T(E) \propto \{1 + r_1 r_2 \exp(-2i\delta_{\mathrm{Pb}}) + r_1 r_3 \exp[-2i(\delta_{\mathrm{Pb}} + \delta_{\mathrm{Ag}})] + r_2 r_3 \exp(-2i\delta_{\mathrm{Ag}})\}^{-1}, \tag{3}$$

where r_1, r_2, and r_3 are the reflectivities at the vacuum, Pb/Ag, and Ag/Si interfaces, respectively, and $\delta = k_\perp Nt + \Phi/2$, which is related to the Bohr-Sommerfeld quantization condition. Aside from the addition of a low-order polynomial, $B(E)$, to account for the background, the product of the absolute square of this interference factor and a smooth low-order polynomial, $A(E)$, describes the photoemission intensity [6]:

$$I(E) = |T(E)|^2 A(E) + B(E). \tag{4}$$

$A(E)$ accounts for variations in the intensity due to photoemission cross-section dependences. An optical potential is included in our model to account for electronic damping due to electron-electron scattering, electron-phonon scattering, and residual defect scattering [6,18,19]; this damping causes the quantum-well peaks to broaden. Partial reflections and transmissions at the Pb/Ag interface allow the electronic structure of the buried Ag quantum well to be detected. Figure 2(b) reveals that the model well describes the observed photoemission spectra over a wide range of Pb coverages. Labeled according to nominal coverages determined by a crystal thickness monitor, each Pb film actually comprises two coverages. For the simulation, the assumed thickness of a given film was 1/3 ML less than the indicated nominal coverage [20].

The interface reflectivities and boundary phase shifts obtained from the simulation are shown in Fig. 3. The reflectivity of the Ag/Si interface r_3 as a function of energy rises rapidly near the Si band edge (~0.5 eV below the Fermi level) and approaches unity within the Si band gap.

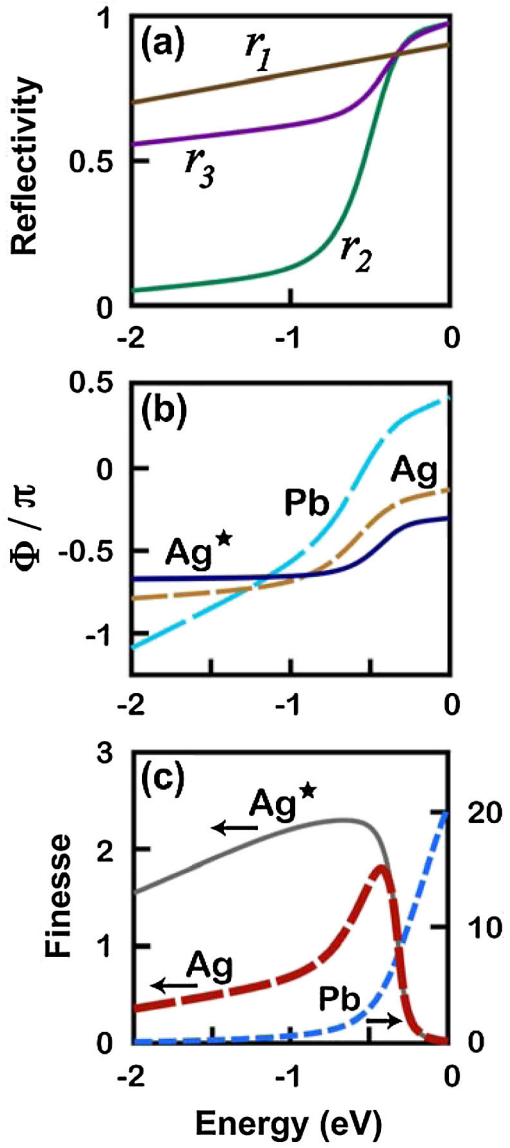

FIG. 3 (color online). (a) The reflectivities corresponding to the Pb/vacuum (r_1), Pb/Ag (r_2), and Ag/Si (r_3) interfaces. (b) The total phase shifts at the two boundaries [see Eq. (1)] associated with films of Pb on Ag, the embedded Ag film, and a bare Ag film (marked with *) on Si(111). (c) The finesse of a bare 25-ML Ag film on Si(111) (solid grey curve marked with *), a 25-ML Ag film on Si(111) covered by a Pb film (long red dashes), and a 5-ML Pb film on a 25 ML Ag film on Si(111) (short blue dashes). The vertical scale of the Pb finesse differs from that of the two Ag curves; the axis relevant to each curve is indicated with an arrow.

The Pb/Ag-interface reflectivity r_2 follows a similar trend, also approaching unity within the Ag L gap. Below the gap, r_2 diminishes rapidly, giving rise to a corresponding decrease in the photoemission intensity of the Ag features at large Pb film thicknesses; this term, though small, remains finite due to the discontinuity in band structure. As the relevant region of the Pb(111) band structure contains no gaps, the reflectivity of the Pb/vacuum interface, r_1, varies smoothly and is well described by an approximately linear function. The phase shift and the reflectivity are both derived from an analytic complex reflection coefficient of the wave function. As such, they are connected by analyticity; the total phase shifts presented in Fig. 3(b) also show sharp changes near the band edges, as expected [21,22]. The total phase shift represents the sum of the phase-shift contributions from the two boundaries of a film. Generally, the reflectivity affects the quantum-well peak widths.

The finesse, $F(E)$, of an interferometer typifies its confinement capability and relates to its quality factor, Q. For either a Pb or Ag film, the finesse is given by

$$F(E) = \frac{\pi\sqrt{r_i r_{i+1}}\exp(-Nt/2\lambda)}{1 - r_i r_{i+1}\exp(-Nt/\lambda)}, \quad (5)$$

where r_i and r_{i+1} are the reflectivities of the ith interface and the mean-free-path λ is related to the aforementioned optical potential. The reflectivities deduced in the above-described simulation determine $F(E)$ for the buried Ag film, allowing for a clear characterization of the electronic behavior within its confines. Figure 3(c) displays calculated curves of $F(E)$ for a bare 25-ML Ag film on Si(111), a 25-ML Ag film on Si(111) covered by a Pb film of arbitrary thickness, and a 5-ML Pb film on a 25-ML Ag film. As expected, $F(E)$ in each case diminishes as $|E|$ increases. The Ag finesse reaches its maximum at the onset of the Ag gap and drops precipitously above the gap, resulting from the inability of electrons to propagate in gaps. Covering the 25-ML Ag film with a Pb film of arbitrary coverage decreases r_2, thereby diminishing the confinement capability of the Ag and causing a stark difference in $F(E)$ for the two cases.

In summary, unambiguous Fabry-Pérot-like behavior observed for Ag films covered by Pb films of thicknesses up to 25 ML (~70 Å) indicates that electronic coherence may endure through overlayers of a wide range of thicknesses relevant to applications. Our results demonstrate that angle-resolved photoemission, despite its long historical reputation as a surface-sensitive probe, is actually able to probe the quantized electronic states in such deeply buried quantum wells. Even though the photoelectrons are ejected only from the near-surface region, the long coherence length of the electron wave function provides the means to sense the system at a much larger depth. This coherence is well maintained through the incommensurate Ag/Pb interface. Acquiring a solid understanding of such quantum-interference effects and behaviors is of paramount importance as technology pursues more complex thin-film architectures.

We thank R. Budakian and M. Stone for insightful comments. This work is supported by the U.S. Department of Energy (Grant No. DE-FG02-07ER46383). We acknowledge the American Chemical Society Petroleum Research Fund and the U.S. National Science Foundation (Grants No. DMR-05-03323 and No. DMR-09-06444) for partial support of the equipment and personnel at the Synchrotron Radiation Center (SRC). The SRC is supported by the U.S. National Science Foundation (Grant No. DMR-05-37588).

[1] T.-C. Chiang, Surf. Sci. Rep. **39**, 181 (2000).
[2] F. J. Himpsel, J. E. Ortega, G. J. Mankey, and R. F. Willis, Adv. Phys. **47**, 511 (1998).
[3] M. Milun, P. Pervan, and D. P. Woodruff, Rep. Prog. Phys. **65**, 99 (2002).
[4] L. Aballe, C. Rogero, and K. Horn, Phys. Rev. B **65**, 125319 (2002).
[5] R. K. Kawakami, E. Rotenberg, E. J. Escorcia-Aparicio, H. J. Choi, J. H. Wolfe, N. V. Smith, and Z. Q. Qiu, Phys. Rev. Lett. **82**, 4098 (1999).
[6] J. J. Paggel, T. Miller, and T.-C. Chiang, Science **283**, 1709 (1999).
[7] L. Bürgi, O. Jeandupeux, A. Hirstein, H. Brune, and K. Kern, Phys. Rev. Lett. **81**, 5370 (1998).
[8] I. B. Altfeder, D. M. Chen, and K. A. Matveev, Phys. Rev. Lett. **80**, 4895 (1998).
[9] A. Weismann, M. Wenderoth, S. Lounis, P. Zahn, N. Quaas, R. G. Ulbrich, P. H. Dederichs, and S. Blügel, Science **323**, 1190 (2009).
[10] M. H. Upton, C. M. Wei, M. Y. Chou, T. Miller, and T.-C. Chiang, Phys. Rev. Lett. **93**, 026802 (2004).
[11] N. J. Speer, S.-J. Tang, T. Miller, and T.-C. Chiang, Science **314**, 804 (2006).
[12] M. H. Upton, T. Miller, and T.-C. Chiang, Phys. Rev. B **71**, 033403 (2005).
[13] K. Shimada, in *Very High Resolution Photoelectron Spectroscopy*, edited by S. Hüfner (Springer, Berlin, 2007), pp. 86–112.
[14] N. W. Ashcroft and N. D. Mermin, *Solid State Physics* (Saunders College, New York, 1976).
[15] T.-C. Chiang, T. Miller, and W. E. McMahon, Phys. Rev. B **50**, 11102 (1994).
[16] N. V. Smith, Phys. Rev. B **32**, 3549 (1985).
[17] O. S. Heavens, *Optical Properties of Thin Solid Films* (Dover, New York, NY, 1965).
[18] L. I. Schiff, *Quantum Mechanics* (McGraw-Hill, New York, 1968).
[19] J. J. Paggel, T. Miller, and T.-C. Chiang, Phys. Rev. Lett. **83**, 1415 (1999).
[20] For example, an indicated nominal Pb coverage of 7 ML represents an actual coverage of 6.7 ML, signifying the presence of both 6-ML and 7-ML coverages.
[21] M. A. Mueller, E. S. Hirschorn, T. Miller, and T.-C. Chiang, Phys. Rev. B **43**, 11825 (1991).
[22] D. A. Ricci, Y. Liu, T. Miller, and T.-C. Chiang, Phys. Rev. B **79**, 195433 (2009).